CANGAROO-II Observations of the PSR B1259−63/SS 2883 Binary System

Akiko Kawachi
ICRR, University of Tokyo, Kashiwa, Chiba 277-8582, Japan
Tsuguya Naito
Faculty of Management Information, Yamanashi Gakuin Univ., Kofu, Yamanashi 400-8575, Japan
for the CANGAROO collaboration

Abstract

The PSR B1259−63/SS 2883 binary system have been observed in the TeV energy region using the CANGAROO-II Cherenkov telescope and the results are reported. The nearby binary consists of a fast rotating radio pulsar and a Be star in a highly eccentric orbit. It has been pointed out that the relativistic pulsar wind and the dense mass outflow of the Be star may emit high energy gamma rays up to TeV energy via inverse Compton scattering process or via decay of neutral pions produced by proton-proton collisions. The observations were performed in 2000 and 2001, during the post-periastron period. Upper limits of ∼0.2–0.5 Crab levels are obtained which constrain the mass outflow parameters of the Be star.

1. Introduction

The PSR B1259−63 is a 48 msec radio pulsar which was found to be in a highly eccentric orbit ($e = 0.87$) with a 10th magnitude Be star, SS 2883 (Johnston et al. 1994). The orbital period is 1236.7 days and the recent periastron was in October 2000 (MJD 51834.51). Through 1994–1996, unpulsed X-ray emissions with a single power-law spectrum have been detected at the six different orbital phases with the *ASCA* satellite (Hirayama et al., 1996, 1999). The spectral index and the luminosity of obtained X-rays are time-variable, however, the consistency at the same orbital phase in different years supports that the observed variation is of binary modulation (Hirayama et al. 1999). The periastron passage in 1994 was also covered by the multiwavelength campaign with *ROSAT, ASCA* and *Compton Gamma Ray Observatory (CGRO)* (Grove et al. 1995). The power-law spectrum extended to 200 keV without pulsation. No emissions in the 1 MeV–3 GeV range were detected. Several TeV observations of the binary were attempted with the CANGAROO 3.8-m telescope (Sako et al. 1997) to result in the marginal $4.8\,\sigma$

pp. 1–7

Table 1. A summary of the observations in this paper.

	Date	θ_{zen} (degree)		Time Real (min.)	Time Effective (min.)
Obs. A	2000/12/01–04	58	ON:	201	196
			OFF:	192	160
Obs. B	2001/3/19–26	34	ON:	1252	623
			OFF:	1122	645

significance of gamma-ray signals at most.

The multiwavelength spectrum around the 1994 periastron strongly suggests that the hard X-ray emissions are originated from synchrotron radiation of non-thermal electrons with Lorenz factor $\Gamma_e = 10^6$–10^7. The electrons released as pulsar wind may be accelerated in the shock wave generated in the region where the relativistic pulsar wind interacts with the dense mass outflow from the Be star. Electrons with such Lorenz factor in a radiative environment of the binary system may produce high energy gamma-rays. Emissions from pulsar wind via inverse Compton (IC) scattering process have been discussed in Kirk et al. (1999) Ball & Kirk (2000) and Shibazaki et al. (2002). In the contact surface of the outflows, ions as well as electrons may be accelerated to high energies due to the first-order Fermi mechanism. If the protons are accelerated efficiently in the shocked region, gamma-ray emissivity from p-p collisions can be dominant over IC scattering process which suffers from Klein-Nishina effect. A new model calculation of the mechanism is applied and discussed in this paper.

2. Observations

The PSR B1259−63/SS 2883 system was observed with the CANGAROO-II Cherenkov telescope (Mori et al. 2001) at the two different orbital phases for several days in December 2000 (*Obs. A*; MJD 51881.7 in average of the observation time) and in March 2001 (*Obs. B*; MJD 51991.5), about 47 days and 157 days after the recent periastron. In the two observation sets, the averaged zenith angles (θ_{zen}) were different; 58° for *Obs. A* and 34° for *Obs. B*, corresponding to the seasonal difference. The target and an offset region were observed for equal amounts of time at each night under moonless conditions. The total observation time of each observation set is summarized in Table 1.

3. Analysis and Results

The charge and the timing information of each PMT signal was recorded for each event. The digitized counts of PMT signal charge were pedestal-subtracted and the variations in the pixel gains were normalized. Accidental events caused mainly by the nightsky were rejected by requiring signals of more than 5 neighboring PMTs above a ∼3.3-photoelectron threshold. The event counting rate satisfying the requirement is almost stable (∼0.6 Hz and 1.9 Hz in *Obs. A* and *Obs. B*, respectively). Data under unstable weather condition were rejected by checking fluctuations in the counting rate. Effective observation time (Table 1) refers to the survived data here. In order to discriminate gamma-ray events from cosmic-ray induced events, a likelihood analysis was applied (Enomoto et al. 2002) to the light images recorded by the camera. We used Monte Carlo simulations (Okumura et al. 2002) for a gamma-ray event set (γ) and the OFF-source events for a background event set (BG). A hit-map weighted by charge digits was fitted with an ellipse using parameters, *width*, *length*, and *distance* (Hillas 1982) to characterize an event. Each of the image parameters were two-dimensionally plotted versus the total digital counts of charge in the image for the γ and BG event sets to deduce probability density functions (PDF) of "gamma-ray like" and "background-like" events, respectively. A single parameter, R_{prob}, of an event was defined as $R_{prob} = Prob(\gamma)/(Prob(\gamma) + Prob(BG))$, where $Prob(\gamma)[Prob(BG)]$ is a probability of being gamma-ray [background] calculated from the PDFs. A selection criteria ($R = 0.4$, $R_{prob} \geq R$) was chosen considering the figure-of-merit of γ to BG events and the γ event acceptance.

After the image selection, events with the image orientation parameter, *alpha* (Punch et al. 1992) less than 20° for *Obs. A* (15° for *Obs. B*) were assumed to be gamma-rays from the pulsar. The smearing effect of the observation zenith angle was considered using simulations. Fig. 1 and 2 show the distributions of *alpha* parameters after all the other cuts were applied. The OFF-source distribution ("OFF") of each observation data set, was normalized to that of ON-source ("ON") by the number of bin contents in *alpha* $\geq 40°$. No statistically significant excess of the "ON" over the "OFF" is seen in the *alpha* histograms of the both observation sets. Subtractions of the normalized "OFF" from the "ON" result in 31 and 47 events within the *alpha* selection criteria which correspond to the significance (assuming Poisson fluctuations only) of 1.0 and $0.6\,\sigma$, respectively for *Obs. A* and *Obs. B*. The total gamma-ray acceptance of the system after the analysis has been estimated based on the simulation for the both observation conditions. The energy threshold (E_{th}) is defined as a median of the acceptance multiplied by the generated energy spectrum and $E_{th} = 3.6\,\mathrm{TeV}$

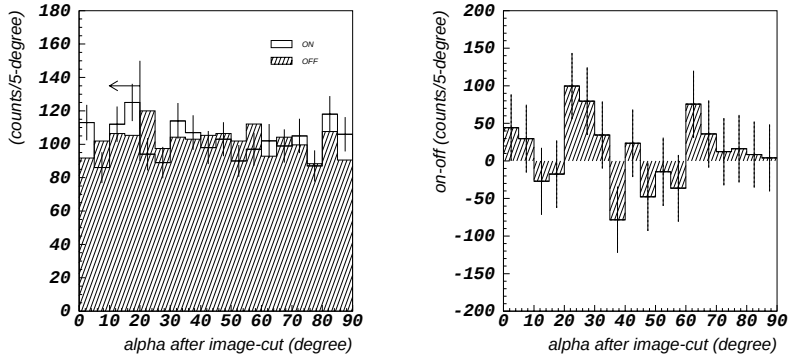

Fig. 1. The distributions of the orientation angle *alpha* (*Obs. A*). (*left*) : "OFF" (hatched) is overlaid "ON" (blank) after the normalization. $alpha \leq 20^o$ are assumed to contain gamma-ray signals from the binary. (*right*) : after the subtraction.

and 0.78 TeV are derived for $E^{-2.5}$ spectra of *Obs. A* and *Obs. B* data sets, respectively. The corresponding effective areas are 3.6 and 1.3 $\times 10^9 \mathrm{cm}^2$. The $2\,\sigma$ upper limits are calculated as $F(\geq 3.6\,TeV) \leq 1.4 \times 10^{-12} \mathrm{cm}^{-2}\mathrm{s}^{-1}$ (*Obs. A*) and $F(\geq 0.78\,TeV) \leq 3.1 \times 10^{-12} \mathrm{cm}^{-2}\mathrm{s}^{-1}$ (*Obs. B*). The whole procedure of analysis was performed changing the simulated spectral index from -2.5 to -2.0. The significance levels of the gamma-ray signals are unchanged, E_{th} and the gamma-ray acceptances increase by about 20 percent for the both observation sets. The systematic error in the absolute energy scale has been estimated to be 15 percent (Okumura et al. 2002).

4. Discussion

The observational results are compared with a model calculation by p-p collision mechanism. It is provided the pulsar wind is driven by the rotational energy loss of the pulsar and the wind pressure is enhanced into the equatorial direction by a factor of 0.1 compared to 4π distribution. For the Be star mass outflow, the density profile ρ is assumed to depend on the distance from the star, R, as $\rho(R) = \rho_0(R/R_*)^{-n}$ with the power-law index n, and the flow speed $v(R) = v_0(R/R_*)^{n-2}$ from conservation of mass flux, where R_* is the star radius and ρ_0 and v_0 are density and speed of the outflow at the surface of the star, respectively. The location of the shock regime is determined by the pressure balance between the pulsar wind (depending on the distance from the pulsar as a power of -2) and the outflow of the star, ρv^2, (depending on the distance from the star as a power of $n-4$). Here we introduce a new parameter, x, defined as $x = \rho_{0,-12} v_{0,6}$, where

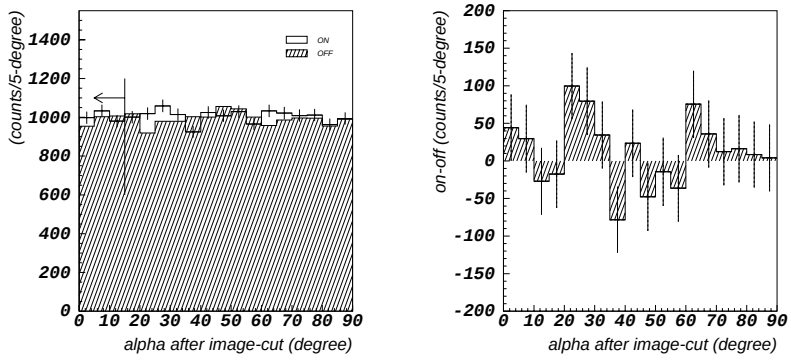

Fig. 2. The *alpha* distributions (*Obs. B*). $(left)$: "OFF" (hatched) is overlaid "ON" (blank) after the normalization. $alpha \leq 15^o$ are assumed to contain gamma-ray signals from the binary. $(right)$: after the subtraction.

ρ_0 and v_0 are expressed in units of 10^{-12}g cm^{-3} and 10^6cm s^{-1}, respectively. We try x = 1000, 3000, and 10000 and n = 2.5 considering the possible ranges of the parameters estimated by early studies of Be stars (Waters et al. 1988). With the assumed compression ratio of 4, the acceleration efficiency of 0.1, and the maximum energy of the accelerated protons of $\sim 10^6$, the energy flux of protons accelerated at the shock is evaluated as a function of energy E_p ($j_p(E_p) \propto E_p^{-2.0}$). Then the gamma-ray spectrum emitted from collisions between the accelerated protons and matter of the Be star outflow has been calculated. The variation of the pressure balance location causes an orbital modulation in the light curve (details of the model is described in Kawachi et al. 2002).

The obtained upper limits are compared with the model light curves (Fig. 3). E_{th} of the results have been scaled to 1 TeV. A light curve (dotted line) calculated by IC scattering process of the un-shocked pulsar wind with the Lorentz factor of 10^7 is taken from Ball & Kirk (2000), however, our upper limits are too large to constrain the model. The predicted gamma-ray light curves by the p-p collision model are integrated (E$\geq$ 1 TeV) for x = 1000, 3000, and 10000. The out flow parameter is constrained as $x \leq 3000$. The constraint is the similar level of the limitation by the X-/gamma-ray results (Tavani & Arons 1997).

5. Summary

We have performed TeV observations of the PSR B1259−63/SS 2883 binary system at the two different orbital phases in the post-periastron period. Upper limits on the integrated gamma-ray flux are obtained. A TeV gamma-ray

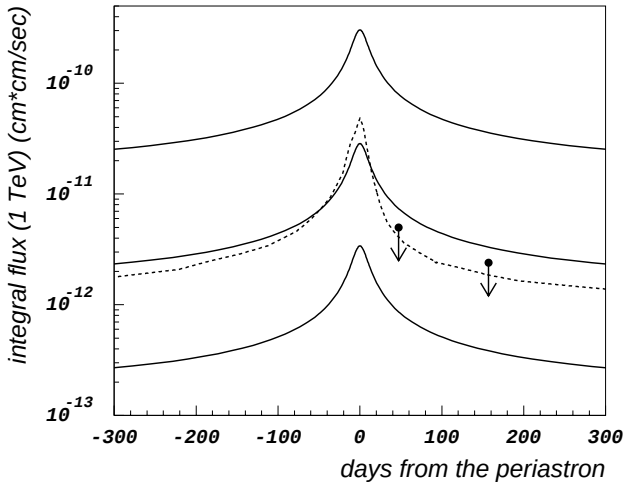

Fig. 3. The upper limits on the integrated gamma-ray flux are compared with the model calculated curves as a function of day after periastron epoch.

emission model by p-p collision mechanism is newly introduced and is discussed with the results which constrain the mass out flow parameters.

6. References

1. Ball L. and Kirk J.G. 2000, Astropart. Phys., 12, 335
2. Enomoto R. et al. 2002, Nature 416, 823
3. Grove J.E. et al. 1995, ApJ 447, L113
4. Hillas A.M. 1982, J.Phys. G 8, 1475
6. Hirayama M. et al. 1996, PASJ 48, 833
7. Hirayama M. et al. 1999, ApJ 521, 718
8. Johnston S. et al. 1994, MNRAS 268, 430
9. Kawachi A. et al. 2002, in preparation
10. Kirk J.G. et al. 1999, Astropart. Phys. 10, 31
11. Mori M. et al. 2001, Proc. 27th ICRC (Hamburg) vol. 5 pp.2831
12. Okumura K. et al. 2002, ApJ 579, L9
13. Punch M. et al. 1992, Nature 358, 477
14. Sako T. et al. 1997, Proc. 25th ICRC (Durban) vol. 3 pp.193
15. Shibazaki T. et al. 2002, In these proceedings, G21
16. Tavani M. & Arons J. 1997, ApJ 477, 439
17. Waters L.B.F.M. et al. 1988, A&A 198, 200